Hindawi Publishing Corporation
Laser Chemistry
Volume 2006, Article ID 10647, 7 pages
doi:10.1155/2006/10647

Research Article

Varnish Ablation Control by Optical Coherence Tomography

Michalina Góra,[1] Piotr Targowski,[1] Antoni Rycyk,[2] and Jan Marczak[2]

[1] *Institute of Physics, Nicolaus Copernicus University, ul. Grudziadzka 5, 87 100 Toruń, Poland*
[2] *Institute of Optoelectronics, Military University of Technology, ul. Kaliskiego 2, 00 908 Warszawa, Poland*

Received 15 September 2006; Accepted 7 November 2006

Recommended by Costas Fotakis

Preliminary results of the application of optical coherence tomography (OCT), in particular in its spectral mode (SOCT) to the control of a varnish ablation process, are presented. Examination of the ablation craters made with an Er:YAG laser allows optimization of the laser emission parameters controlling fluence with respect to efficiency and safety of the ablation process. Results of measurements of ablation crater depth as a function of the number of pulses for a given fluence are presented for selected resins. This validates the applicability of SOCT to calibration of ablation conditions for the particular laser-varnish-paint layer combinations, and of its usage in planning the varnish ablation procedure. These results also imply that a review of conventional ablation thresholds is called for. Applicability of the SOCT technique to contemporaneous in situ monitoring of the range of varnish ablation is discussed.

1. INTRODUCTION

The cleaning of painted surfaces is one of the most crucial operations in art conservation. The protective varnish layer must be removed, if it has turned yellow or opaque, or it covers old, darkened retouchings which are to be removed during the conservation process. Extremely high precision and selectivity is essential for this task in order to preserve the original paint layers without modifying their original colours. Among traditional methods of paint removal, the mechanical one is the safest, but requires undue patience, especially when it must be applied either to a very thin and inhomogeneous layer or to foreign deposits. Chemical methods based on toxic solvents are very difficult to control (even when they are applied in the form of swab or gel), because the solvent may penetrate the paint layer and cause risk of damage during the next steps of conservation. Furthermore, the materials that should be removed are, in the great majority of cases, insoluble in media that are tolerated by paint layers. In addition, substances that are not harmful to the paint layer are usually not aggressive enough to remove the varnish layer.

According to contemporary methods of art conservation, the most desirable requirement is contemporaneous control of varnish removal. This complicated task is difficult to achieve with the traditional empirical methods of art restoration.

Laser techniques are becoming important tools in the conservation (restoration, diagnostic, and protection) of cultural heritage. Research on laser cleaning of paintings and icons by an excimer laser was initiated at the Foundation for Research and Technology-Hellas in Greece [1]. The interested reader can find a comprehensive literature on conservation techniques based on the application of lasers in the proceedings of LACONA conferences I to VI. The cleaning of works of art and historical objects with lasers allows selective removal of undesirable layers, leaving the original paint layer intact [1–4]. A significant problem connected with laser ablation is online monitoring and in situ control during each stage of the laser cleaning. A very useful technique is laser induced breakdown spectroscopy (LIBS) [5, 6] in which the chemical composition of the plasma produced is spectroscopically analyzed, and traces of paint components indicate that the cleaning beam has reached the paint layer. Contemporaneously with matters related to monitoring the cleaning process, phenomena occurring in ablated material, such as the formation of microcracks, defects, and other structural changes, are being investigated. Other nondestructive optical methods, for instance, holographic interferometry [7], have already been successfully used for this purpose.

In this contribution, the preliminary results of the application of optical coherence tomography (OCT) to the control of a varnish ablation process are presented. The OCT method allows noncontact and nondestructive imaging of semitransparent objects. It enables fast and convenient calibration of ablation conditions for the particular laser-varnish combination. Moreover, the technique provides information on the volume of removed material and the thickness, structure, and quality of the remaining varnish layer. This is essential for control of the ablation depth. In this paper, the results of ablation of different varnishes by the Er:YAG laser (working in the so-called short free-running regime) are presented.

2. EXPERIMENT

The use of the laser for varnish removal needs precise optimization of its conditions. Ablation with minimum thermal damage of adjacent areas depends on the absorption parameters of the material, together with the laser pulse energy and duration, and the thermal relaxation time of the material, that is, the time needed for diffusion of heat in the substance. Additionally, multiple scattering in matt surfaces, when present, significantly increases absorption of the laser radiation. Therefore, the major parameter of the laser pulse to be established is the radiation fluence. This parameter should be determined experimentally for each combination of varnish and paint layers. This test is usually performed near the edge of the painting. Unfortunately, the parameters obtained within the test area are not usually optimal for other areas. This necessitates a method which may ultimately be used for contemporaneous monitoring of the ablation process in situ.

To assay the ability of OCT to monitor the varnish removal process, model samples of varnish layers were prepared by applying selected resins to fused silica plates (see samples section). Without wetting the surface, a cumulative number of impulses of the same fluence were applied to consecutive locations in the sample. As a result, a set of graded craters was produced. Generally, two kinds of OCT analysis of ablation craters are possible: qualitative, when it is mainly the shape of craters in varnish layer (surface map) which is recovered, and quantitative, when additionally the depths of the ablation craters are measured. Together, these enable estimation of the material removed. Independently, scanning electron microscope (SEM) images (Novoscan 30, Zeiss, Germany) of sample surfaces were obtained to compare to the surface maps generated from volume OCT data. It is worthwhile to note that, since samples have to be gold-plated for this purpose and examined in vacuum, the SEM method cannot be applied in situ.

3. MATERIALS AND METHODS

3.1. Er:YAG laser system

An essential prerequisite for laser cleaning is the proper choice of laser wavelength. This depends on the absorption coefficient of the material to be ablated. In the experiments

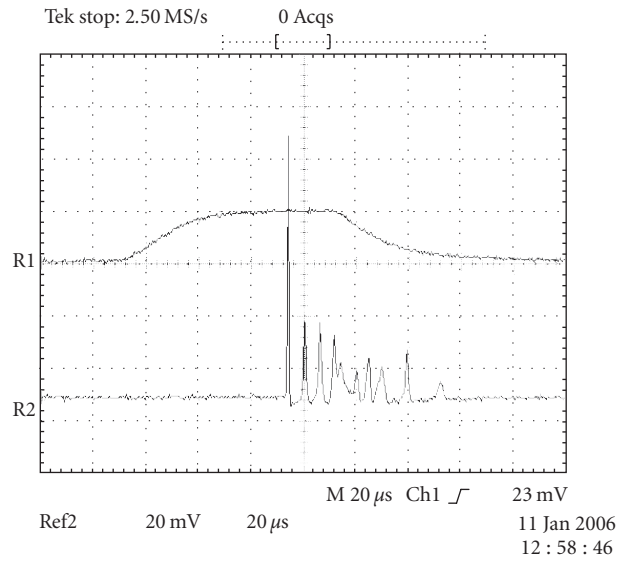

Figure 1: Time course of the pumping impulse (upper curve), and of the laser pulse (burst pulse) which usually consists of dozen or so pulses of free-running generation, each lasting for about 1 microsecond.

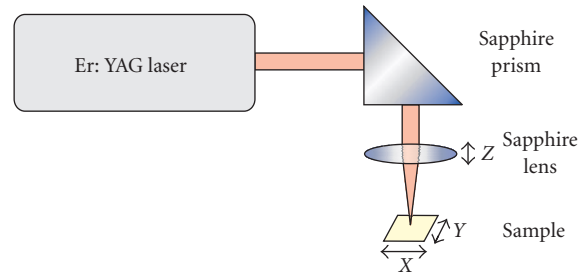

Figure 2: Diagram of the Er:YAG laser setup used in this study.

described, an infrared Er:YAG laser working at a wavelength of 2.936 μm was used to ablate various varnish layers from fused silica plates. Radiation of this wavelength is strongly absorbed by the OH bond vibration (the absorption coefficient can reach a value of as high as $10^5\,\mathrm{cm}^{-1}$), so that the depth of penetration of light into the treated medium may be extremely small [8, 9]. OH groups can be introduced onto the surface of layers to be removed as a liquid, for example, water or alcohol, film. However, this treatment (called wetting) has not been used in the presented study.

The Er:YAG laser was working in the short free-running mode (or burst mode), in which several impulses of free generation were emitted, each of them lasting for about 1 microsecond, the total duration of the burst being less than 80 microseconds (see Figure 1). The total output energy of the laser was adjustable, but always kept below 80 mJ. The fluence can be controlled by means of the focusing optics (prism and lens, both made of sapphire, Figure 2).

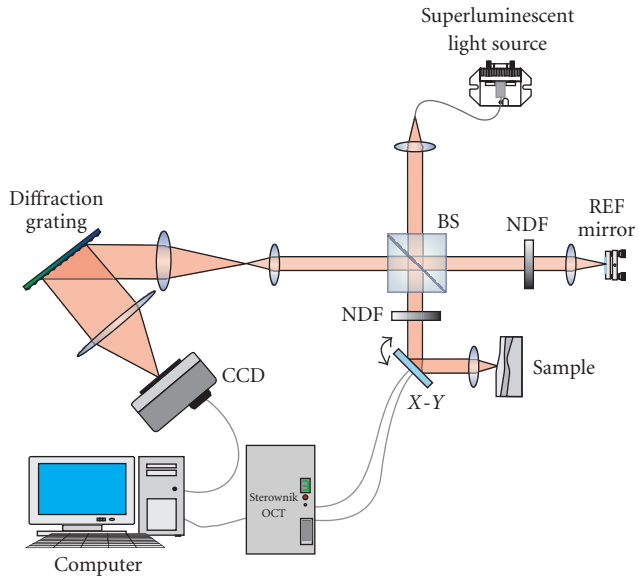

FIGURE 3: Diagram of the SOCT instrument used in the study: BS—beam splitter, NDF—neutral density filter, CCD-CCD line-scan camera, X-Y-galvanometric scanner.

3.2. Optical coherence tomography

Optical coherence tomography (OCT) is a new, fast-developing technique for noncontact, nondestructive imaging of semitransparent objects. In this method, the positions of scattering and/or reflecting interfaces in the internal structure of the object along the penetrating beam are obtained. OCT has found its main applications in medicine, but it has also been successfully used in materials science, particularly for museum objects. Among these, it has already been shown that OCT is capable of imaging varnish layers [10–12]. A comprehensive review of this last application, as well as a general idea of operational procedures, are given elsewhere in this volume [13].

The Spectral OCT (SOCT) system shown schematically in Figure 3 is a bulk optics instrument based on a Michelson interferometer setup. The superluminescent diode (Superlum Ltd., Russia) emitting light with a central wavelength of 835 nm and spectral width (FWHM) of 50 nm was used as a light source. The beam of light, of high spatial but low temporal coherence, is split into two interferometric arms with the aid of a 50 : 50 nonpolarising beam-splitting cube BS. One arm is terminated by the reference mirror kept in a fixed position. The other, namely, the object arm, comprises a set of two transversal scanners X-Y (Cambridge Technology Inc., USA) which are used for scanning the probing beam across the object. The beam is focused on the object by a lens L and penetrates the object. Some of it is scattered and/or reflected back from elements in its structure, and this is finally collected by the same optics L, and returned to the beam-splitter BS. It is then combined with the light returning from the reference arm. The resulting interference signal is analyzed and registered by a spectrometer (comprising a holographic diffraction grating: 1800 grids, Spectrogon AB, Sweden, and a CCD line scan camera: 1024 pixels, 8 bit A/D conversion, Dalsa Corporation, Canada). The detection conditions were set up to the shot-noise limited mode in order to utilise whole dynamic range of the CCD camera. The spectral fringe patterns registered by this detector are then transferred to a personal computer. The fringe pattern signal is then reverse Fourier transformed into one line of a tomogram (an A-scan). The exposure time per A-scan is usually 30 microseconds.

The axial resolution of the system is $\sim 6\,\mu$m in these media which have refractive indices ranging from 1.3 to 1.5. The transversal resolution is kept below $15\,\mu$m. In order to obtain either a 2D slice (B-scan) or a 3D (volume) tomogram, the beam is scanned transversally by galvanometric scanners X-Y.

The total data collection time for a B-scan composed of 5000 A-scans is thus 0.15 second, and about 5 seconds is required for 3D (volume) data.

The signal is visualised in real time as a cross-sectional view and stored for postprocessing. The numerical processing of the data, besides the reverse fast Fourier transform, essential to the SOCT method, includes: subtraction of noninterference background, spectral shaping [14], and numerical dispersion correction [15].

In the 2D OCT tomograms or B-scans (see Figures 6(e), 6(f), and 7 in the results section), the intensity of light reflected or scattered from the interfaces along the penetrating beam is coded in a false-colour scale: warm colours (red and yellow) indicate a high scattering level of the probing light, while the cold ones (blue and black) indicate low scattering levels. Light is incident from the top, and the narrow line indicates the strong reflecting surface of intact varnish. Areas altered by the ablation process produce multiple scattering and are visible as fuzzy regions of mixed colour.

The OCT volume data may be used, *inter alia*, to recover the surface profile of the object examined (Figures 6(c) and 6(d)). In this process, the position of the first nonzero signal in each A-scan, corresponding to the first scattering boundary (the air-object interface), is automatically determined.

3.3. Samples

For the OCT experiments, five resins were selected to model varnishes of different properties: polyester resin in styrene with and without SiO_2 as matting agent, vinyl resin, polyurethane resin, and epoxy resin. All resins were applied to fused silica plates (Vitrosil 005^{TM}, one inch diameter and two millimetres thick). The transmission of the plate is $\sim$ 91% at 2,936 μm. The laser energy meter, placed after the plate, was used to indicate independently the total ablation of the resin.

4. RESULTS AND DISCUSSION

4.1. Estimation of the ablation conditions

To establish safe conditions for the removal of the varnish layer (Winsor & Newton Matt Varnish) from wooden

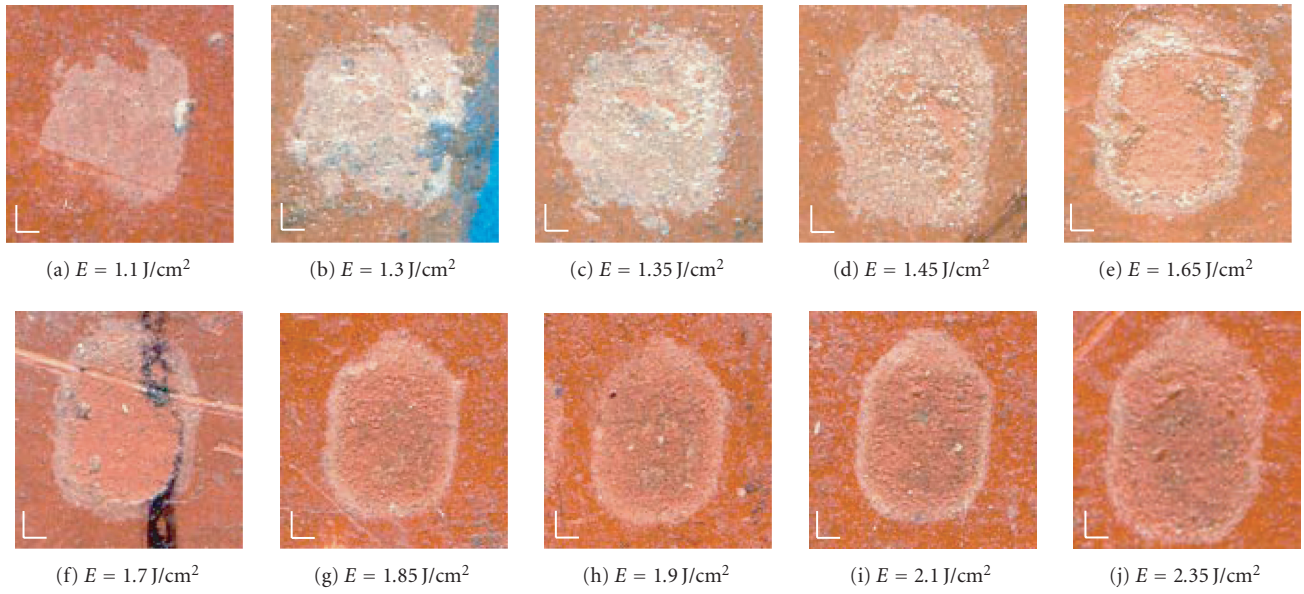

(a) $E = 1.1\,\mathrm{J/cm^2}$ (b) $E = 1.3\,\mathrm{J/cm^2}$ (c) $E = 1.35\,\mathrm{J/cm^2}$ (d) $E = 1.45\,\mathrm{J/cm^2}$ (e) $E = 1.65\,\mathrm{J/cm^2}$

(f) $E = 1.7\,\mathrm{J/cm^2}$ (g) $E = 1.85\,\mathrm{J/cm^2}$ (h) $E = 1.9\,\mathrm{J/cm^2}$ (i) $E = 2.1\,\mathrm{J/cm^2}$ (j) $E = 2.35\,\mathrm{J/cm^2}$

Figure 4: Illustration of the reaction of the varnish and underlying paint layer to different laser fluences. Bars indicate 1 mm in both directions.

Figure 5: Result of ablation of varnish (Winsor & Newton Matt Varnish) over different underlying paint layers using the same fluence ($1.7\,\mathrm{J/cm^2}$).

Table 1: Ablation thresholds estimated by inspection of the sample surface.

Resin	Ablation threshold $\mathrm{J/cm^2}$
Polyester resin in styrene with SiO_2 as a matting agent	3.3
Polyester resin in styrene without matting agent	3.3
Vinyl resin	2.9
Polyurethane resin	4.3
Epoxy resin	2.9

polychrome, a sequence of test ablations was performed. In Figure 4, the results of single-pulse ablations with fluences ranging from $1.1\,\mathrm{J/cm^2}$ (the ablation threshold) to $2.35\,\mathrm{J/cm^2}$ are presented. Inspection of the ablation spots leads to estimation of the optimal range of fluences as between $1.45\,\mathrm{J/cm^2}$ and $1.7\,\mathrm{J/cm^2}$. On exceeding $1.7\,\mathrm{J/cm^2}$, carbonization of the paint layer sets in.

However, as can be seen in Figure 5, the fluence suitable for varnish removal from the red paint is not sufficient in a different area of the object, where the underlying paint is green. Therefore, each such different area of the object should be treated individually to avoid unnecessary damage.

For all model samples, the ablation threshold was estimated by inspection of the effects of a single pulse on the sample surface. The fluence was increased until a change in the resin surface was visible. The results are summarised in Table 1.

4.2. OCT assay of the ablation process

To prepare objects for OCT examination, a set of graded craters was produced by directing cumulative numbers of impulses of the same fluence to consecutive locations in the sample (as described in Section 2). In these experiments, two sets of craters were created for each sample: one with a fluence of $4\,\mathrm{J/cm^2}$ (Figure 6(a)), the other with a fluence of $7\,\mathrm{J/cm^2}$ (Figure 6(b)).

As can be seen from Figure 6, there is excellent correspondence between the microphotographs and the surface profiles obtained with OCT. However, extra useful information may be obtained from the OCT tomograms. Firstly, the surface profile is clearly visible, allowing tracking of the ablation process: the depth of crater was chosen as an indicator of progress. Secondly, the range of alteration of the structure of material under the crater surface is seen—this feature is not accessible with SEM. Thirdly, it is clearly visible when the whole layer is burnt through (Figure 7).

The results obtained for all of the samples are summarised in Figure 8. As can be seen from the diagram, the depth of crater usually increases almost linearly with the number of pulses. In that case, it is possible to calculate the number of pulses necessary exactly to ablate the required layer of varnish.

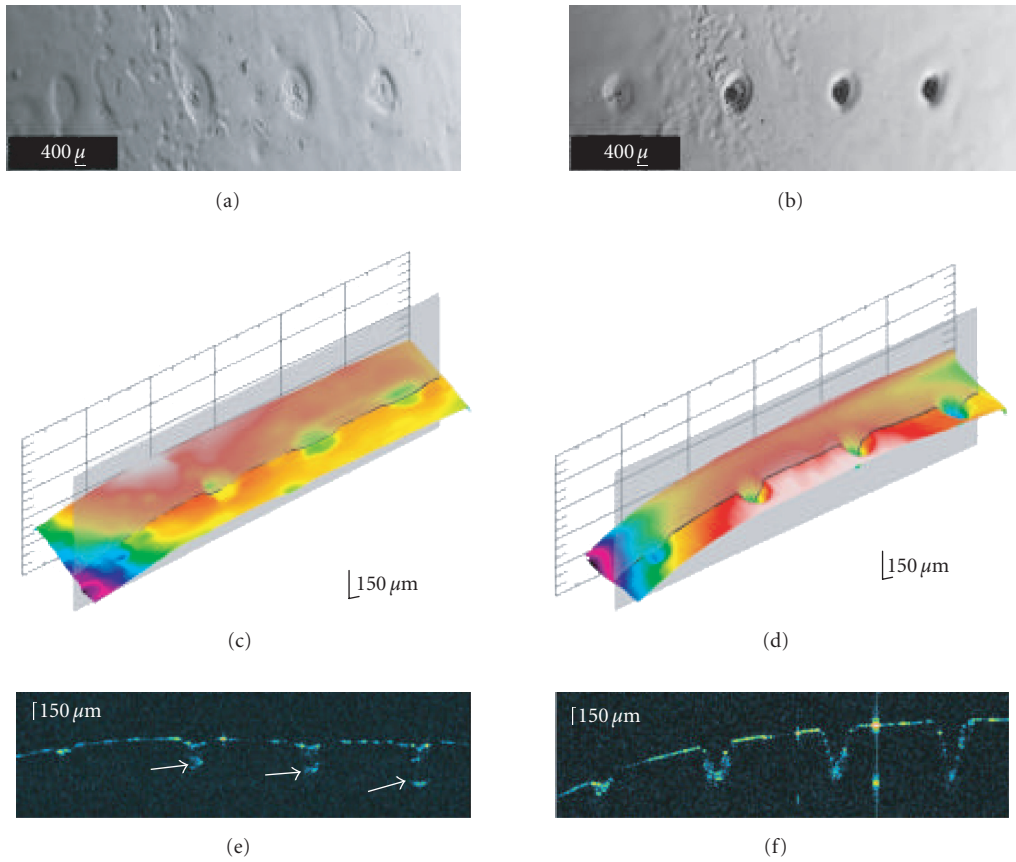

FIGURE 6: Testing of ablation conditions of Polyester resin in styrene without matting agent with two irradiation fluences: (a,c,e) 4 J/cm^2 and (b,d,f) 7 J/cm^2. In both cases, craters were formed by accumulation of 1, 2, 5, and 10 laser pulses (from the left to the right). Upper panels: SEM surface microphotographs; middle panels: surface maps recovered from OCT data—gray planes indicate positions where the OCT tomograms were taken; lower panels: the OCT tomograms (B-scans). Notice the expanded vertical scale for both the OCT surface maps and the OCT tomograms.

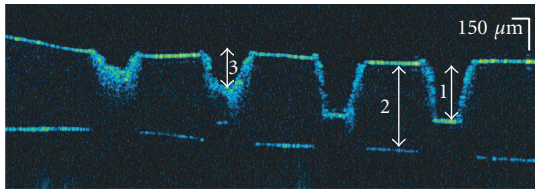

FIGURE 7: The OCT tomogram of the ablation of polyester resin in styrene with SiO_2 as a matting agent using a fluence of 7 J/cm^2. Craters were formed by accumulation of 1, 2, 5, and 10 laser pulses (from the left to the right). Craters formed by 5 and 10 pulses reach the substrate surface, and determination of putative crater depth is not possible. Notice the discrepancy between the thickness of the resin layer in the craters (1) and in the resin itself (2). This arises because of refraction in the resin, and vertical distances recovered by OCT are optical ones. The bars indicate distances in the air, to define properly the crater depth (3).

However, for some media (here, the polyester resin with or without the matting agent) pulses of higher fluence create deeper ablation craters, whereas consecutive pulses of low fluence do not increase the crater depth. On the other hand, the presence of a shallow crater in these cases indicates that some thermal process has occurred (Figures 6(a), 6(c), and 6(e)): the varnish material only melts, then resolidifies. This process causes some changes to the structures underneath the crater which can be seen as regions of higher scattering in the OCT tomograms (Figure 6(e), arrows). The presence of such microdefects underneath the surface of the target material has previously been reported by Bonarou et al. [7]. However, it is worthwhile to note that this graded growth of structural defects with increasing number of laser pulses occurs also below threshold, when the varnish surface remains almost intact. It seems that, even though the value of the fluence is higher then the conventional ablation threshold given in Table 1, ablation does not in fact occur. Therefore, the ablation threshold obtained in the conventional way for this resin is probably underestimated.

5. CONCLUSIONS

The cleaning of painted surfaces is one of the most critical operations in art conservation. The application of lasers

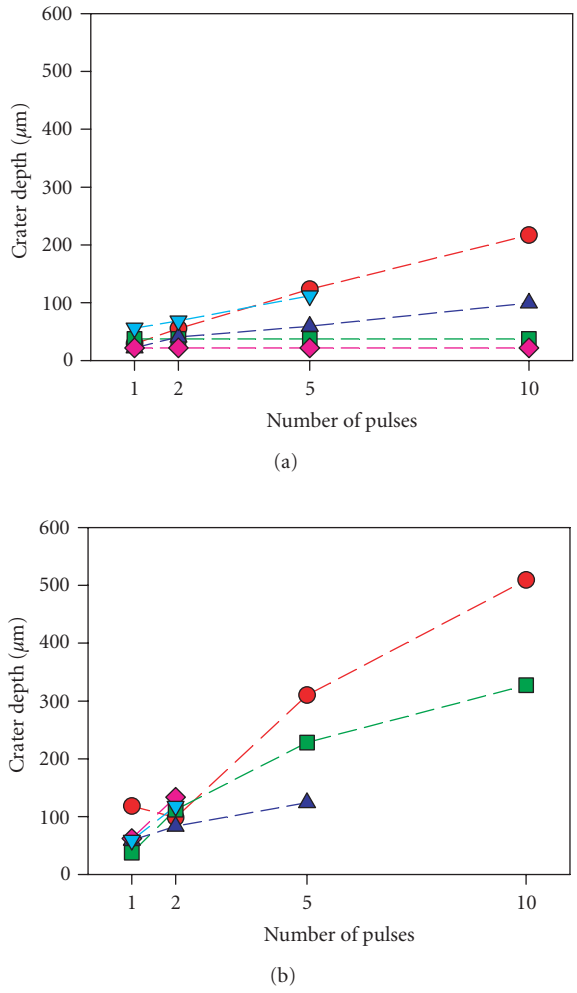

FIGURE 8: Depth of ablation craters obtained with cumulative number of pulses of fluence (a) 4 J/cm^2 and (b) 7 J/cm^2. ♦ polyester resin in styrene with SiO_2 as matting agent; ■ polyester resin in styrene without matting agent; ▲ vinyl resin; ▼ polyurethane resin; ● epoxy resin.

for this task requires precise optimization of the operating conditions. However, these conditions may differ in different parts of the object. The OCT method presented enables fast and convenient calibration of ablation conditions for particular laser-varnish-paint layer combinations, and it may be used to plan the varnish ablation procedure. It also permits nondestructive, in situ estimation of ablation speed and/or instantaneous monitoring of the thickness of remaining material. This is essential for the control of the ablation range. The spectral modality of the OCT technique (SOCT) best suites this task due to its high speed. In SOCT, the major limitation is the data processing speed if real-time monitoring is of the essence. Current moderately priced personal computers permit image processing at the rate of up to 10 medium resolution frames per second. This appears to be fast enough for the lasers used for ablation, which have pulse or burst repetition rates of up to a few Hz. It is therefore expected, despite its physical limitations, that SOCT will be instrumental for instantaneous, in situ control of varnish ablation.

ACKNOWLEDGMENTS

This work was supported by Polish Ministry of Science Grant 2 H01E 025 25. Authors wish to thank Dr. Robert Dale for very valuable discussions and Dr. Janusz Szatkowski for SEM images.

REFERENCES

[1] C. Fotakis, D. Anglos, C. Balas, et al., "Laser technology in art conservation," in *OSA TOPS on Lasers and Optics for Manufacturing*, A. C. Tam, Ed., vol. 9, pp. 99–104, Optical Society of America, Washington, DC, USA, 1997.

[2] J. F. Asmus, "Light cleaning: laser technology for surface preparation in the arts," *Technology and Conservation*, vol. 3, no. 3, pp. 14–18, 1978.

[3] M. Cooper, Ed., *Laser Cleaning in Conservation: An Introduction*, Butterworth Heinemann, Oxford, UK, 1998.

[4] J. Marczak, "Renovation of works of art by laser radiation," *Przegląd Mechaniczny*, vol. 15-16, pp. 37–40, 1997.

[5] D. Anglos, S. Couris, and C. Fotakis, "Laser diagnostics of painted artworks: laser-induced breakdown spectroscopy in pigment identification," *Applied Spectroscopy*, vol. 51, no. 7, pp. 1025–1030, 1997.

[6] Final Report CRAFT project ENV4-CT98-0787, "Advanced workstation for controlled laser cleaning of artworks," http://www.art-innovation.nl/.

[7] A. Bonarou, L. Antonucci, V. Tornari, S. Georgiou, and C. Fotakis, "Holographic interferometry for the structural diagnostics of UV laser ablation of polymer substrates," *Applied Physics A: Materials Science and Processing*, vol. 73, no. 5, pp. 647–651, 2001.

[8] A. de Cruz, M. L. Wolbarsht, and S. A. Hauger, "Laser removal of contaminants from painted surfaces," *Journal of Cultural Heritage*, vol. 1, supplement 1, pp. 173–180, 2000.

[9] A. Andreotti, P. Bracco, M. P. Colombini, et al., "Novel applications of the Er:YAG laser cleaning of old paintings," http://www.art-restorers-ass.nl/.

[10] P. Targowski, B. Rouba, M. Wojtkowski, and A. Kowalczyk, "The application of optical coherence tomography to nondestructive examination of museum objects," *Studies in Conservation*, vol. 49, no. 2, pp. 107–114, 2004.

[11] H. Liang, M. G. Cid, R. G. Cucu, et al., "En-face optical coherence tomography—a novel application of non-invasive imaging to art conservation," *Optics Express*, vol. 13, no. 16, pp. 6133–6144, 2005.

[12] I. Gorczyńska, M. Wojtkowski, M. Szkulmowski, et al., "Varnish thickness determination by spectral optical coherence tomography," in *Proceedings of the 6th International Congress on Lasers in the Conservation of Artworks LACONA VI, Vienna, Austria 2005*, J. Nimmrichter, W. Kautek, and M. Schreiner, Eds., Springer, Berlin, Germany, 2006.

[13] P. Targowski, M. Góra, and M. Wojtkowski, "Optical coherence tomography for artwork diagnostics," *Laser Chemistry*, vol. 2006, Article ID 35373, 2006.

[14] M. Szkulmowski, M. Wojtkowski, P. Targowski, and A. Kowalczyk, "Spectral shaping and least square iterative deconvolution in spectral OCT," in *Coherence Domain Optical*

Methods and Optical Coherence Tomography in Biomedicine VIII, vol. 5316 of *Proceedings of SPIE*, pp. 424–431, San Jose, Calif, USA, January 2004.

[15] B. Cense, N. A. Nassif, T. C. Chen, et al., "Ultrahigh-resolution high-speed retinal imaging using spectral-domain optical coherence tomography," *Optics Express*, vol. 12, no. 11, pp. 2435–2447, 2004.